

HELICOPTER DYNAMIC COMPONENT FATIGUE LIFE PREDICTION WITH A PROBABILISTIC LOAD AND STRENGTH MODEL

Sam Dekker
Airbus Helicopters Germany
Delft University of Technology
Industriestraße 4,
D-86609 Donauwörth
Germany

Georg Wurzel
Airbus Helicopters Germany
Industriestraße 4,
D-86609 Donauwörth
Germany

René Alderliesten
Delft University of Technology
Kluyverweg 1, 2629 HS Delft
the Netherlands

ABSTRACT

Fatigue life is a random variable. The reliability of a conservative fatigue life prediction for a component in the helicopter dynamic system thus needs to be substantiated. A standard analytical substantiation method uses average manoeuvre loads instead of seeing manoeuvre loads as a random variable whose distribution is estimated with limited precision. This simplification may lead to inaccuracies. A new simulation-based method is developed to conservatively predict fatigue life while also accounting for the full random distribution and uncertainty of manoeuvre loads. Both methods fully account for uncertain fatigue strength but assume that the mission profile is known or can at least be conservatively estimated. Simulations under synthetic but realistic engineering conditions demonstrate that both methods may be used for accurate substantiation of conservative fatigue life predictions. The simulations also demonstrate that, under the tested conditions, uncertainties from manoeuvre loads may be neglected in fatigue life substantiations as the resulting error is not significant with respect to uncertainties in component fatigue strength.

1 INTRODUCTION

Failure of components in the helicopter dynamic system, such as the main rotor mast or the levers that control the angle of attack of main rotor blades, may have catastrophic consequences. The period between crack initiation and component failure is usually too short to detect a crack in time during inspection intervals. Such components thus need to be replaced before the probability that a large crack initiates becomes too high. Rotorcraft certification according to FAR 27.571 or FAR 29.571 by means of AC 27-1B MG11 requires providing appropriate fatigue life substantiation for each of these components. If necessary, an upper limit to the time a component can be used is set by a fixed Service Life Limit (SLL).

Fatigue life of a component can be predicted when one knows how fatigue damage accumulates (i.e. Palmgren-Miner hypothesis), the component's fatigue strength (i.e. S-N curve) and the loads during life (i.e. load spectrum).

The exact fatigue strength of a specific component is never known in advance. Scatter in, for example, material properties, dimensioning, machining or other manufacturing processes demands that fatigue strength be considered as a random variable.

The loads that a component experiences during its life depend on numerous variables, for example, the type of missions that are flown, how these missions are executed (i.e. speed, duration, number and type of manoeuvres etc.), the precise technique of the pilot(s) executing the manoeuvres, the weight and centre-of-gravity of the helicopter during the manoeuvres, or even the meteorological conditions. The loads that occur during life must thus be regarded as a random variable as well.

Clearly, the fatigue life of a specific component cannot be predicted exactly but must also be considered as a random variable. For certification, it is common to show that the probability of a fatigue failure during the specified maximum service life of a randomly selected component in the fleet is not higher than a certain probability, e.g. $P_{fia}(SLL) = 10^{-6}$.

The load spectrum that a component is subjected to during its life may be decomposed into two random variables. First, the mission profile (i.e. the sequence and timeshare of turns, hovers, landings etc.) and second the loads that occur when flying a manoeuvre (e.g. the maximum load during landing is likely to be between 85N and 260N).

A common standard analytical method to predict a conservative fatigue life simplifies manoeuvre load distributions to only their averages and derives its full reliability substantiation from the distribution of component strength. Such a method thus assumes that uncertainty in manoeuvre loads is negligible with respect to uncertainty in fatigue strength. The validity of this assumption is however not obvious and may not be general. This paper therefore introduces a new simulation-based method to predict fatigue life while also accounting for the full random distribution and uncertainty of loads. Both methods assume that the mission profile is known or can at least be conservatively estimated.

The two methodologies are applied to a realistic but artificial fatigue life prediction problem. It is demonstrated that under the conditions of this problem, errors do arise from not fully accounting for uncertainty in manoeuvre loads. However, it is also demonstrated that these errors are in practise insignificant and that it is therefore allowed

to represent manoeuvre load distributions only by their averages.

2 ANALYTICAL FATIGUE LIFE PREDICTION

A baseline standard analytical fatigue life prediction methodology is outlined here. This analytical method is similar to the approved lifetime prediction methods applied by Airbus Helicopters Germany for rotorcraft dynamic components. This simple to apply method is characteristic for industry practise. Section 4 later introduces a newly developed simulation-based method that features more complexity but promises higher accuracy.

2.1 Fatigue damage accumulation model

A fatigue damage accumulation model is needed to predict fatigue life for given component strength and loads during life. The model employed here is widely used (e.g. Schijve 2009 [1]) and consists of:

- A Weibull-type S-N curve that defines the number of load cycles until fatigue failure under constant amplitude loading:

$$(2.1) \quad \sigma_a(N)|_R = \sigma_{a_e} + \frac{\sigma_{a_{ult}} - \sigma_{a_e}}{\left[\frac{(\log_{10} N)^\beta}{\alpha} \right]}$$

where: σ_a is the applied stress amplitude (at stress ratio R); N is the number of load cycles (until failure); σ_{a_e} is the stress amplitude of the endurance limit or fatigue limit (at stress ratio R); $\sigma_{a_{ult}}$ is the ultimate stress amplitude determined by: $\sigma_{a_{ult}} = \sigma_{ult} \cdot \frac{1-R}{2}$ where σ_{ult} is the ultimate stress; R is the stress ratio $\frac{\sigma_{min}}{\sigma_{max}}$; $\{\alpha, \beta\}$ are component specific Weibull curve parameters.

- The Goodman-relation to translate load cycles to the stress ratio for which the S-N curve is valid:

$$(2.2) \quad \sigma_a(R) = \frac{\sigma_{a_{ult}} \cdot \sigma_a|_{R_i}}{\sigma_{a_{ult}} - \sigma_m|_{R_i} \cdot \frac{1+R}{1-R}}$$

where: $\sigma_a|_{R_i}$ and $\sigma_m|_{R_i}$ are the stress amplitude and mean stress of the i^{th} load cycle class respectively

- Rainflow counting (according to ASTM E1049-85) preceded by Peak-Valley (PV) filtering to determine the number of cycles in each load cycle class (load spectra are discretized)

- The Palmgren-Miner linear damage accumulation hypothesis to define fatigue failure under spectrum loading:

$$(2.3) \quad \text{Fatigue failure} \equiv \sum \frac{n_i}{N_i} = 1$$

where: n_i is the number of load cycles in the i^{th} load cycle class; N_i is the number of cycles until fatigue failure under constant amplitude load defined by the i^{th} load class

2.2 Random strength model

As fatigue strength is a random variable, both the shape and position of the S-N curve can be considered as uncertain. While ignoring shape variations, the following S-N-P curve is used to model random fatigue strength:

$$(2.4) \quad \sigma_a(N)|_R = SF|_{\hat{\sigma}} \cdot \left\{ \hat{\sigma}_{a_e} + \frac{\hat{\sigma}_{a_{ult}} - \hat{\sigma}_{a_e}}{\left[\frac{(\log_{10} N)^\beta}{\hat{\alpha}} \right]} \right\}$$

The strength factor SF is a random variable distributed according to a lognormal distribution (as a transformation of an associated standard normal distribution N):

$$(2.5) \quad p(SF | \hat{\mu}, \hat{\sigma}) = e^{\{\hat{\sigma} \cdot N(\hat{\mu}=0, \hat{\sigma}=1) + \hat{\mu}\}}$$

$\{\hat{\sigma}_{a_{ult}}, \hat{\sigma}_{a_e}, \hat{\alpha}, \hat{\beta}\}$ are Maximum Likelihood Estimates (MLEs) of the S-N curve parameters, given component static test results and/or component constant amplitude fatigue tests.¹ As the strength distribution (i.e. the distribution of SF) should have its mean equal the expected S-N curve, $\hat{\mu}$ must be zero, so that the mean strength factor value equals one.

Since the strength factor is assumed independent of N (i.e. homoscedastic noise assumption), it is allowed to translate all fatigue test results used to fit the S-N curve to an arbitrary N . It is then straightforward to obtain $\hat{\sigma}$, the MLE of the standard deviation of strength.

With the full S-N-P curve defined, a conservative working curve can be derived. For example, if the working curve should represent the fatigue strength of the (on average) weakest component out of one million randomly selected components, then SF can be computed according to:

$$(2.6) \quad SF(P_{fail} = 10^{-6}) = e^{\{\hat{\sigma} \cdot N^{-1}(\hat{\mu}=0, \hat{\sigma}=1, P_{fail}) + \hat{\mu}\}}$$

¹ The embellishments above symbols only distinguish different parameters for which equal symbols are used.

with N^{-1} denoting the inverse Cumulative Distribution Function (CDF) of the normal distribution.

Figure 2.1 and Figure 2.2 illustrate such a working curve.

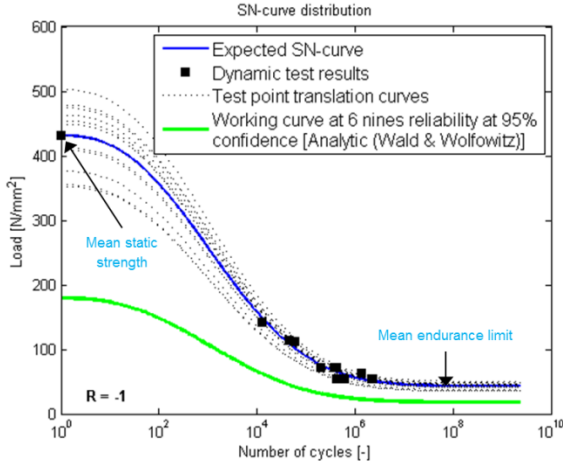


Figure 2.1: Example of constant amplitude fatigue test results, the MLE S-N curve and conservative working curve for a component from the dynamic system.

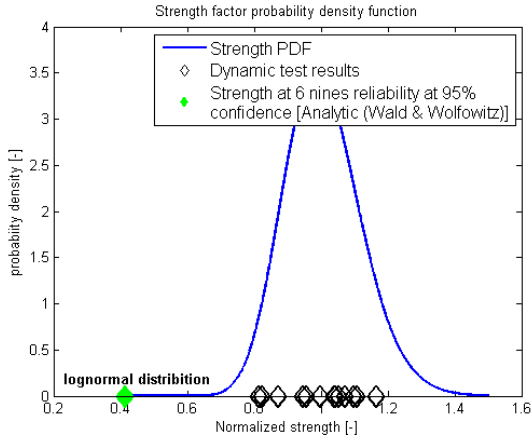


Figure 2.2: Exemplary fatigue test results (normalized by the MLE S-N curve), the derived MLE estimate of the PDF of normalized fatigue strength (SF), and the strength factor corresponding to the conservative working curve.

It is impossible to make a perfect estimate of the S-N-P curve as only a limited number of fatigue tests can be done. Therefore it is considered that the estimate of the Probability Density Function (PDF) of the SF itself, and thereby also the conservative strength quantile (2.6), is imperfect. To account for this uncertainty, a confidence interval for the conservative SF quantile (2.6) is computed. (i.e. to require a 95% upper single sided confidence level here means that, if the set of fatigue tests would be repeated many times, then 95% of the conservative SF estimates, one for each new set of fatigue test results, would really meet a 0.999 reliability requirement. The remaining 5% conservative SF estimates would in fact correspond to a probability of failure that would be higher

than 10^{-3}). (e.g. Hahn & Meeker [2] further explain confidence intervals)

Both the mean $\hat{\mu}$ and standard deviation $\hat{\sigma}$ (of the associated normal distribution) of the strength factor SF (2.5) must thus be considered as random variables and are distributed according to: [2]

$$(2.7) \quad p(\hat{\mu} | \hat{\mu}, \hat{\sigma}, n_{test}) = t\left(\bar{\mu} = \hat{\mu}, \bar{\sigma} = \frac{\hat{\sigma}}{\sqrt{n_{test}}}, \bar{\nu} = n_{test} - 1\right)$$

$$(2.8) \quad p(\hat{\sigma} | \hat{\sigma}, n_{test}) \propto \hat{\sigma} \cdot \sqrt{\frac{n_{test} - 1}{\chi^2(\bar{\nu} = n_{test} - 1)}}$$

where: $t(\bar{\mu}, \bar{\sigma}, \bar{\nu})$ denotes the Student t-distribution; $\chi^2(\bar{\nu})$ is the Chi-squared distribution; both with $\bar{\nu}$ degrees of freedom; n_{test} denotes the number of test results that are available to fit the S-N-P curve.

The conservative strength factor for the working curve at a reliability level $1 - \gamma$ (i.e. $1 - 10^{-3}$) and a lower single sided confidence level α (i.e. 95%) can be computed by: [3]

$$(2.9) \quad SF(\gamma, \alpha | \hat{\mu}, \hat{\sigma}, n_{test}) = \exp\left\{\hat{\mu} - \sqrt{\frac{n_{test} - 1}{inv \chi^2(P_{fail} = 1 - \alpha | \bar{\nu} = n_{test} - 1)}} \cdot r(\gamma, n_{test}) \cdot \hat{\sigma}\right\}$$

with:

$$(2.10) \quad r(\gamma, n_{test}) = \frac{1}{\sqrt{n_{test}}} - N^{-1}(P_{fail} = \gamma | \bar{\mu} = 0, \bar{\sigma} = 1)$$

2.3 Load model

The loads during the service life are represented by a load spectrum that is cycle counted from a load sequence. Ideally, this load sequence would be the continuous load signal measured on the component during its life. In practise though, an (conservatively) estimated load spectrum is used instead.

The first step in obtaining this load spectrum is to define a set of manoeuvres that cover how the helicopter can be flown. For example: A: take-off; B: level flight; C: hover; etc. Using these regimes, a mission profile can be made. This mission profile sets how much time (percentage) the helicopter spends in each manoeuvre, e.g. [A: 3%; B: 80%; ...], and in which sequence the manoeuvres are flown per unit of time, e.g. [A C B F B ...] every 100 flight hours (FH).

In practise, this mission profile is generally based on pilot and operator surveys as well as experience. In any case, it must be conservative for all helicopters in the fleet for which fatigue life is predicted.

Test flights with a specially instrumented helicopter may in practise provide continuous recordings of component loads during the manoeuvres. The same manoeuvres are generally flown multiple times to, for example, cover variations in manoeuvre execution.

The fatigue damage that is accumulated during a flight is computed with a load spectrum of the type as in Figure 2.3.

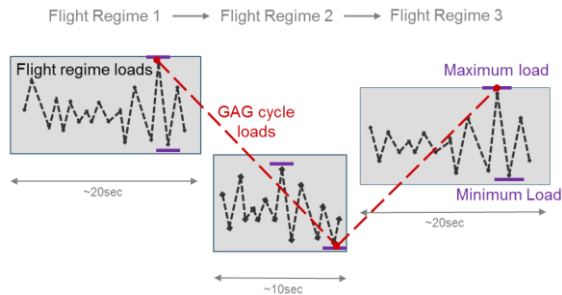


Figure 2.3: Manoeuvre (flight regime) loads and Ground-Air-Ground loads. These loads together make out the full load spectrum.

The total (fatigue relevant) load spectrum for a flight is thus the summation of the load spectra of each flight regime and the load spectrum from the Ground-Air-Ground (GAG) load sequence. The GAG load sequence accounts for the transitions between the manoeuvres and is the most severe load signal that goes through the extreme (i.e. minimum or maximum) load in each manoeuvre.

There is uncertainty regarding the manoeuvre loads and regime extreme loads when predicting the loads during the full fatigue life. In case of the manoeuvre loads, the measured load spectra (one for each time the manoeuvre was flown during test flights) are averaged and scaled to a reference time, i.e. 100FH. The extreme loads from multiple instances are also simply averaged. Inserting these averages into the conservative mission profile (and according to the model in Figure 2.3), leads to the average load spectrum per unit of time.

2.4 Perfect modelling assumption

It is further assumed that the outlined models for fatigue damage accumulation, random fatigue strength and loads are perfect, i.e. do not introduce additional uncertainties. This is in line with standard practise in rotorcraft industry and in compliance with AC 27-1B MG11.

2.5 Substantiated fatigue life prediction

The Service Life Limit is set according to a maximum allowed probability of fatigue failure during the service life, e.g. $P_{fail}(SLL) = 10^{-6}$. SAE ARP4761 specifies reliability requirements as a probability of failure per flight hour and not per service life. It is a 'rule-of-thumb' to multiply $P_{fail}(SLL)$ by 10^{-3} when converting a probability of fatigue failure per service life to per flight hour.

For example, the standard analytical method substantiates a SLL with a probability of failure of $10^{-9}/FH$ at a 95% single sided upper confidence level with the following:

- A working curve with $\gamma = 10^{-6}$ and $\alpha = 0.95$ in (2.9).
- A load spectrum according to a conservative mission profile and average manoeuvre (extreme) loads.

It is thus assumed that all reliability can be substantiated by the working curve. Note that it is in general not possible to derive reliability from the conservative mission profile. The reliability requirement must be met for all helicopters and for all flight hours. If reliability would be derived from conservatism in the mission profile then the reliability requirement would only be met for (at most) averagely demanding operators (i.e. it would be met for VIP operators but not for Search & Rescue).

3 STATE-OF-THE-ART IN PROBABILISTIC FATIGUE LIFE PREDICTION

Questions have been raised during the last decades on the accuracy of the reliability substantiation in standard fatigue life predictions, for example by Lombardo & Fraser [4]. Obviously, the assumption of perfect (or at least conservative) modelling of fatigue damage accumulation can be questioned. However, to the best of the authors' knowledge, there has so far been no systematic attempt to compute accuracy bounds for these models. This is also outside the scope of this paper. The influence on predicted fatigue life of uncertainties in mission profile and regime loads has however been researched before.

Thompson & Adams [5] were one of the first in the rotorcraft industry to extensively model the reliability of SLLs. They included the combined uncertainty from variance in component strength, regime loads and mission profiles in a reliability substantiation model by using a Basic Monte Carlo (BMC) simulation and a random strength, load and usage model. For the random load model, the average load spectrum per regime and also the statistical distribution of regime maximum loads was computed from results of dedicated flight tests. The regime load spectrum was assumed linearly proportional to the maximum load, i.e. when a maximum load is drawn that is twice the average, then the corresponding spectrum is the average spectrum but with the number of cycles multiplied by two. Not accounting for GAG loads and assuming that helicopters randomly change mission profile every $10^3 FH$, the percentage of time spent in each regime is set as a random variable as well (based on extensive usage data). Their (random) strength model was similar to the model in section 2.2. Due to the low efficiency of BMC for aerospace typical low failure probabilities it was necessary to estimate these probabilities by tail extrapolation of a distribution fit through a limited number of BMC samples.

This work was extended by Zhao & Adams [6,7] where use was made of Importance Sampling preceded by First and Second Order Reliability Modelling (FORM/SORM) to first estimate the critical failure region in the parameter space.

Benton [8] and others [9,10,11,12] have all introduced (semi-)analytical fatigue life reliability substantiation models. These all require specifying a PDF for the amplitude and number of cycles of every load case (i.e. constant amplitude loading block) to be considered and also made use of a random strength model similar to section 2.2. This framework is displayed in Figure 3.1.

All previous work on fatigue life prediction reliability substantiation confirmed the importance and value of explicit and combined modelling of uncertainty in strength, loads and usage. Thompson & Adams used their work to re-confirm their standard fatigue life design methodology.

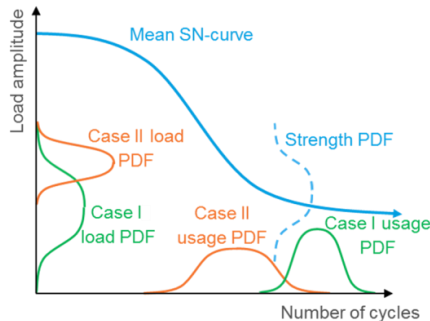


Figure 3.1: Schematic of the random model framework for recent (semi-)analytical SLL reliability models (shown with two load cases).

The following limitations in previous work are however identified:

- It is challenging to model situations of complex spectrum loading, i.e. as in Figure 2.3, in the framework of current (semi-) analytical methods (i.e. as in Figure 3.1).
- The manoeuvre load model of Thompson & Adams, effectively bounds the maximum spectrum load to the highest load measured in test flights. In practise it is however observed that the extreme load during a manoeuvre can be considered as an unbounded random variable. Due to the non-linearity of the S-N curve, PV filtering and range counting, it is expected that only scaling of the number of cycles in a reference spectrum will generally not accurately reflect random variations in manoeuvre damage. E.g. even when considering a spectrum with only one cycle, then doubling the maximum load of this cycle can have a much different effect on manoeuvre damage than doubling the count of this cycle.
- None of the work set out to present tolerance intervals (i.e. confidence intervals on quantiles), despite the high uncertainty associated with

probabilistic fatigue life predictions derived from few statistical samples.

4 SIMULATION-BASED SUBSTANTIATION

A new simulation-based methodology to substantiate fatigue life predictions for critical components in the helicopter dynamic system is presented. This new method aims to meet the following main requirements:

- Model combined uncertainty from loads and strength
- Applicable to problems of very high dimension (i.e. mission profiles with many manoeuvres)
- Suitable up to very low failure probabilities (i.e. 10^{-9})
- Improve accuracy and generality with respect to previously introduced models
- Provide tolerance intervals
- Feature reasonable computational costs

4.1 Modelling assumptions

The following fundamental assumptions are made in the development of this model:

- Perfect fatigue modelling (see section 2.4)
- Helicopters' mission profile is known or can be conservatively assumed and can be modelled as in section 2.3.
- Flight regime loads are independent (i.e. an abnormal high load in a turn to the left is uncorrelated to the load in a next right turn)

The practical implementation of the model presented also assumes that regime loads are identical throughout the fatigue life. (i.e. all turns are flown identically) This practical assumption is expected to promote variance in lifetime and thus to be conservative (i.e. loads do not average-out during life). This feature can however easily be lifted and is not a necessary condition for practical use of the proposed model.

4.2 Modelling of random variables

The substantiation model features an independent probabilistic strength model and a strength-dependent combined probabilistic manoeuvre load & fatigue damage model which is similar to the model used by the virtual fatigue damage accumulation sensor from Dekker et.al. [13].

4.2.1 Stochastic fatigue strength model

The implemented random fatigue strength model is equal as in 2.2. Note that as the proposed substantiation model is simulation-based, the new methodology may easily be adapted to accommodate other (shape-invariant homoscedastic) strength models.

4.2.2 Stochastic load spectrum model

Ideally, manoeuvre loads can be modelled in full and with only a small number of random parameters. (i.e. by means of Fourier decomposition and/or Principle Component

Analysis) It was found that especially in complex and dynamic manoeuvres, the high frequency content of load signals is most relevant for fatigue damage modelling. Unfortunately, there is often not enough flight data available to reliably derive the high number of model parameters that would be necessary to properly include these high frequency load signal features.

However, it was found that modelling of the fatigue damage that is equivalent to the full load signal during a manoeuvre is easier than attempting to model the full load signal. Distribution fits through large samples with synthetically generated flight regime load sequences showed that, for a given S-N curve, and given that there is at least one half-cycle above the endurance limit, the flight regime fatigue damage follows a generalized extreme value (GEV) distribution.

The GEV distribution of a parameter x is defined as follows:

(3.1)

if $\tilde{k} \neq 0$ then:

$$p(x | \tilde{k}, \tilde{\mu}, \tilde{\sigma}) = \frac{1}{\tilde{\sigma}} \exp \left[- \left(1 + \tilde{k} \frac{x - \tilde{\mu}}{\tilde{\sigma}} \right)^{-\frac{1}{\tilde{k}}} \right] \left(1 + \tilde{k} \frac{x - \tilde{\mu}}{\tilde{\sigma}} \right)^{-1 - \frac{1}{\tilde{k}}}$$

else:

$$p(x | \tilde{k}, \tilde{\mu}, \tilde{\sigma}) = \frac{1}{\tilde{\sigma}} \exp \left[- \exp \left(- \frac{x - \tilde{\mu}}{\tilde{\sigma}} \right) - \frac{x - \tilde{\mu}}{\tilde{\sigma}} \right]$$

where $[\tilde{k}, \tilde{\mu}, \tilde{\sigma}]$ are distribution parameters.

The magnitude of the minimum and maximum load that occurs within a manoeuvre is also described by a generalized extreme value distribution. Again, distribution fits through large samples with synthetically generated manoeuvre load sequences, but as well as through available test flight data, are in agreement with this choice.



Figure 4.1: Pie chart showing how probable it is that there are load cycles within a particular manoeuvre above the endurance limit (Z) or not (NZ).

A random model that represents the load model as in Figure 2.3 can now be established, for a given fatigue strength, by defining for each manoeuvre:

- The probability that the loads within the flight manoeuvre cause fatigue damage. This can easily be estimated by computing the fatigue damage for each available manoeuvre sample and computing the ratio between the number of times the manoeuvre was flown with and without damage. A visualization of a resulting binomial distribution is shown in Figure 4.1. This feature circumvents a discontinuity in the manoeuvre damage distribution. Due to the endurance limit, many manoeuvre instances may not cause any manoeuvre damage at all, whereas the damage of the damaging instances is GEV distributed.
- If there is no regime damage, a multivariate probability density function for the minimum and maximum load during the manoeuvre. Such a distribution is shown in Figure 4.2.
- Or, if there is manoeuvre damage, a multivariate PDF for manoeuvre damage and extreme loads. Figure 4.3 shows an example of such a distribution.

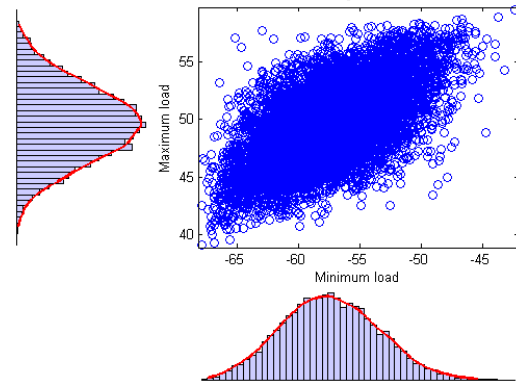


Figure 4.2: A large sample from a fitted multivariate flight regime minimum and maximum load distribution. (i.e. manoeuvre damage is zero) The corresponding marginal distributions are also shown.

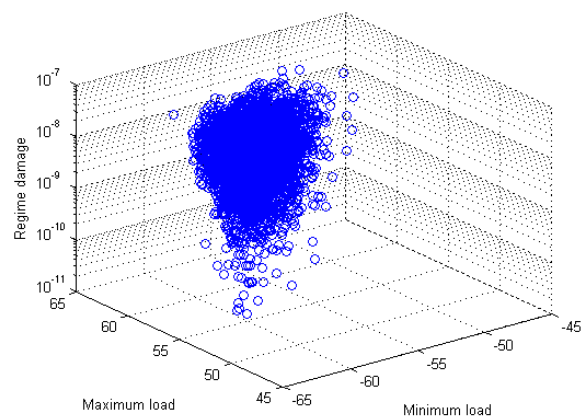


Figure 4.3: A large sample from a fitted multivariate flight regime damage and extreme load distribution.

The multivariate distributions in the practical implementation of the model are realized by t -copulas (Genest & Favre [14]). An alternative implementation by means of Nataf transformation (Hurtado [15]) resulted in

non-conservatively biased and inaccurate results according to an idealized and synthetic verification test. (Such a verification test is described in section 5.2.2)

4.3 Review of reliability estimation methods

The reliability of a Service Life Limit is one minus the probability that a component (in the fleet for which the SLL is valid) experiences a fatigue failure before it reaches the SLL:

$$(3.2) R(\text{SLL}) = 1 - P_{\text{fail}}(\text{SLL}) \quad \text{with failure} \equiv L < \text{SLL}$$

Considering that the fatigue life L is a function of the random parameter vector ω (i.e. containing the sampled strength factor and sampled loads and damages of the manoeuvres), the following indicator function $I(\dots)$ can be defined:

$$(3.3) I[L(\omega)] = \begin{cases} 1 & \text{if } L(\omega) < \text{SLL} \\ 0 & \text{otherwise} \end{cases}$$

Analytically, P_{fail} can now be computed as:

$$(3.4) P_{\text{fail}}(\text{SLL}) = \int_{\Omega} I[L(\omega) | \text{SLL}] \cdot p(\omega) \cdot d\omega$$

However, such an integral over the parameter space Ω is not expected to be mathematically tractable for the model in section 4.2.

4.3.1 Practical numerical reliability estimators

The most intuitive way to estimate $P_{\text{fail}}(\text{SLL})$ is by a BMC estimator:

$$(3.5) P_{\text{fail}}(\text{SLL}) = \frac{1}{n_{\text{sim}}} \sum_{i=1}^{n_{\text{sim}}} \{I[L(\omega_i) | \text{SLL}]\} \quad \text{as } n_{\text{sim}} \rightarrow \infty$$

which is simply drawing a large number, n_{sim} , of parameter vectors from the parameter PDF $p(\omega)$, computing the corresponding fatigue lives and then the fraction of parameter vectors that produce a fatigue life lower than the SLL.

The coefficient of variation (CoV) of a BMC estimate of P_{fail} approximately approaches:

$$(3.6) \text{CoV}_{P_{\text{fail}}} = \frac{\sigma_{P_{\text{fail}}}}{\mu_{P_{\text{fail}}}} = \sqrt{\frac{1 - P_{\text{fail}}}{P_{\text{fail}} \cdot n_{\text{sim}}}}$$

The estimation error is thus proportional to $1/\sqrt{n_{\text{sim}}}$ and independent of the dimension of Ω . This is a highly advantageous feature as the dimension of the parameter vector according to the model in section 4.2 is generally high. However, when the precision of the estimate needs

to have a CoV of 30%, then it is required to evaluate approximately $10/P_{\text{fail}}$ BMC samples. This means that estimating an aerospace typical small P_{fail} becomes highly impractical due to the very large number of samples that need to be evaluated.

Importance Sampling [15] is a common technique to improve the efficiency of the BMC estimator. However, this requires defining a special sampling distribution around the critical region (i.e. where $L(\omega) \approx \text{SLL}$).

Improperly setting this special sampling distribution may cause large errors in the estimate of P_{fail} . The model in section 4.2 dictates a high dimension and complexity of the parameter space. Setting a proper sampling distribution is thus difficult and importance sampling was therefore judged as an unattractive solution method.

Traditionally, reliability problems have been solved semi-analytically by First and Second Order Reliability Methods [15]. These methods are however only accurate under strict conditions, require transformation of the parameter space to a (multivariate) standard normal distribution (e.g. by Nataf transformation) and their computational costs are strongly dependent on the dimension of Ω . Application of FORM/SORM was therefore also judged unattractive.

Most other studied methods, such as BMC acceleration by statistically 'learned' indicator functions (e.g. Kriging [16] or Support Vector Machines [15]) or very recent Particle Algorithms [17] were also considered unappealing, mainly due to their complexity and difficulties due to the high dimensionality of Ω .

4.3.2 Subset Simulation

The method of choice that is implemented to estimate P_{fail} is Subset Simulation (SS) and was developed by Au & Beck [18]. The core concept is to divide a difficult problem of estimating a total probability of failure into multiple sub-problems that are by themselves easy to solve. Considering the CoV of the BMC estimator (3.6), then it shows that estimating a, for example, 1/10 probability of failure can be done with reasonable accuracy while using 'only' one hundred samples, independent of the dimension of the parameter space. Subset Simulation exploits this benefit by estimating the total probability of failure by multiplication of a sequence of conditional high failure probabilities.

A set of intermediate failure events can be defined such that:

$$(3.7) F_1 \supset F_2 \supset \dots \supset F_m = F$$

This means that the failure event $F_m \equiv L < \text{SLL}_m$ is a subset of the (more probable) intermediate failure event

$F_{m-1} \equiv L < SLL_{m-1}$, which is in turn a subset of the (even more probable) intermediate failure event $F_{m-2} \equiv L < SLL_{m-2}$, and so further.

The total probability of failure is now:

$$P_{fail} = P_{fail,1} \cdot \prod_{j=2}^m P_{fail,j} |_{F_{j-1}} \quad (3.8)$$

Here, $P_{fail,1}$ is the probability of the first intermediate failure event F_1 . And $P_{fail,j} |_{F_{j-1}}$ is the probability of failure event F_j , given that (the more probable) failure event F_{j-1} occurs.

Computation of $P_{fail,1}$ can be done straightforwardly by a BMC estimator, especially when the (first) intermediate failure event F_1 is set such that $P_{fail,1}$ equals an easy to compute probability γ , i.e. 1/10. Now, a limited number of samples are drawn, i.e. one hundred, and the fatigue life is predicted for each of these samples. The intermediate failure event F_1 is then defined such that $P(SLL_1 > L) = \gamma$. I.e. the first intermediate limit state SLL_1 , or intermediate failure boundary (an implicit hyper-surface in Ω), is set such that ten out of one hundred of the initial samples lie in the first intermediate failure domain.

A similar procedure can be followed for the subsequent (intermediate) failure events. Again making use of a simple BMC estimator, it is now however necessary to generate samples that are part of the intermediate failure domain F_{j-1} . Generation of a random sample that is conditional on the domain F_{j-1} can be done with Modified Metropolis Hastings Markov Chain Sampling (see [18] for a detailed description).

Additional intermediate failure events are added until the actual SLL for which P_{fail} needs to be known is reached. Figures 4.4, 4.5 and 4.6 show an example of computing $P_{fail}(SLL, s_i)$ by subset simulation.

4.4 Estimating the reliability of a SLL

The load model from section 4.2.2 causes that the PDFs for regime damage and extreme load are dependent on the fatigue strength s , which is itself a random variable. Therefore, P_{fail} should be computed according to:

$$(3.9) \quad P_{fail}(SLL) = \int p_{fail}(SLL, s) \cdot p(s) \cdot ds \approx \sum_i^{n_{bin}} [P_{fail}(SLL, s_i) \cdot P(s_i)]$$

The discretized integral is evaluated by discretizing the strength distribution into i intervals (bins) and while assuming that within each strength interval:

- Regime damage is constant and according to the lowest strength value in the interval

- Correlations between regime extreme loads (and regime damage) are invariant

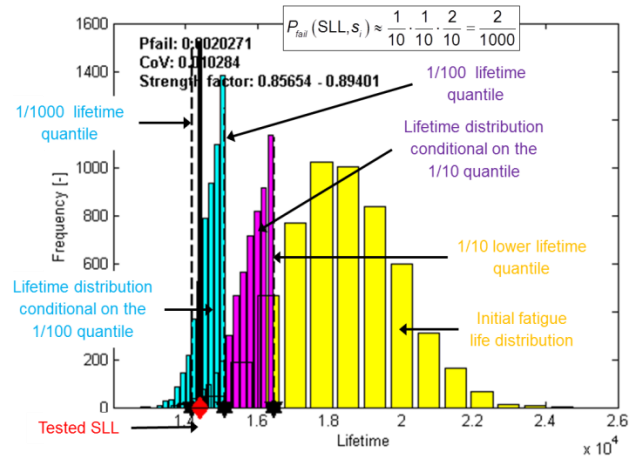


Figure 4.4: Example of Subset Simulation where it takes three intermediate failure events (black stars) to reach the SLL under evaluation (red diamond). The initial lifetime sample is in yellow, the lifetime distribution conditional on F_1 is purple and the lifetime distribution conditional on F_2 is light blue. $P_{fail}(SLL, s_i) \approx 0.1 \cdot 0.1 \cdot 0.2 = 0.002$

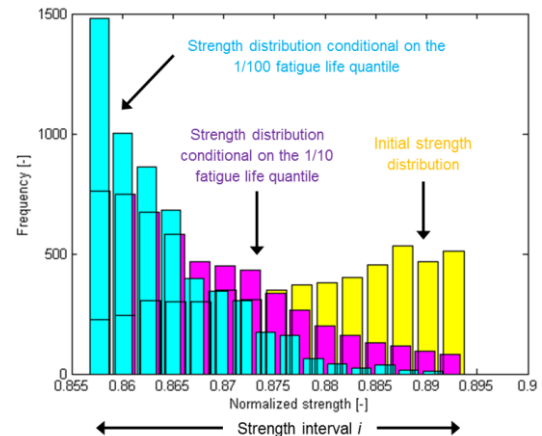


Figure 4.5: Strength samples from SS from the example in Figure 4.4. Note that the strength generally decreases as the intermediate failure events become less probable.

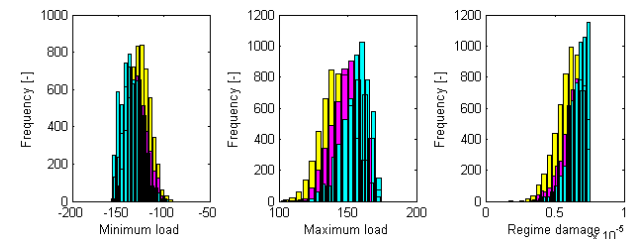


Figure 4.6: SS samples of the minimum load, maximum load and regime damage of a flight regime from the example in Figure 4.4. Note that, for example, the maximum load (middle) generally increases with less likely intermediate failure events, as would be expected.

The parameter PDFs are now fixed for each strength interval. The strength PDF in one such interval is as in Figure 4.7. Note that in general, the coarser the strength discretization grid, the more conservative the estimates of

P_{fail} , as regime damage is consistently overestimated. This was confirmed by simulations under both ideal and small sample size conditions. Although high imprecision may arise if too few samples per subset are used in combination with a very coarse strength grid.

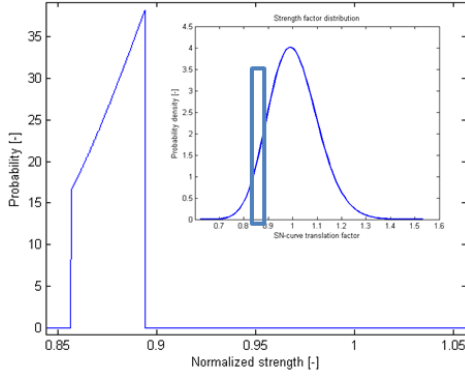


Figure 4.7: Example of strength PDF that is conditional on a strength interval (upper right thick blue box)

4.5 Confidence interval on SLL reliability

In practise, the number of fatigue tests and flight tests that can be done is limited. Also, computational resources are generally limited so that, for example, the sample sizes used in Subset Simulation must be limited. This means that both the parameter distributions themselves, as well as computational results from (3.8), are actually subject to significant uncertainty. It is assumed that other sources of uncertainty (i.e. establishing of the copulas) can be neglected or are conservatively hedged.

Confidence intervals on P_{fail} are computed by (non-)parametric bootstrapping [19]. Essentially, this means that P_{fail} is computed for several alternative variants of the strength, regime extreme load and regime damage distributions and for several alternative SS estimates. Thus, a distribution for P_{fail} can be estimated and, for example, the upper 95th percentile of P_{fail} can be selected for the upper single sided 95% confidence interval. An example is shown in Figure 4.8.

Au and Beck [18] provide an algorithm to estimate the coefficient of variation $CoV_{P_{fail,i}}$ for $P_{fail}(SLL, s_i)$ in (3.9), while assuming that $P_{fail}(SLL, s_i)$ is normal distributed.

The standard deviation of P_{fail} can then be estimated as:

$$(3.10) \quad \hat{\sigma}_{P_{fail}} = \sqrt{\sum_i^{n_{bin}} [CoV_{P_{fail,i}} \cdot P_{fail}(SLL, s_i) \cdot P(s_i)]^2}$$

This feature is important as it allows using small sample sizes in SS (i.e. for low computational costs) while still ensuring conservatism.

Alternative regime loads are determined by non-parametric bootstrapping (i.e. random ‘reshuffling’ with allowing duplicates) of the available manoeuvre load tests

results. Note that standard literature indicates that non-parametric bootstrapping is inaccurate and generally not conservative for small sample sizes. This was also confirmed by extensive simulations by the authors. Nevertheless, it is assumed that this inaccuracy is negligible, i.e. small in comparison to variance due to parametric bootstrapping of the estimated strength distribution. Previous sensitivity studies, e.g. by Zhao & Adams, show that fatigue strength is (much) more influential than manoeuvre loads in fatigue life prediction and thereby support this assumption.

Alternative strength factor distributions are simply drawn from the parameter PDFs (2.7) and (2.8) (i.e. parametric bootstrapping, which the authors confirmed to be accurate by means of extensive simulations).

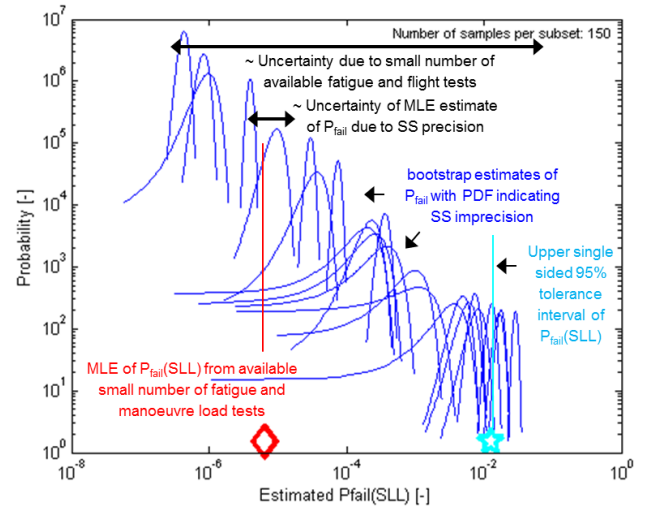


Figure 4.8: Example of the PDFs of bootstrap estimates of $P_{fail}(SLL)$. The width of a PDF represents uncertainty due to limited SS accuracy and the variance in the mean of the different PDFs represents uncertainty due a low number of fatigue and manoeuvre load tests. It demonstrates that imprecision from SS is small with respect to uncertainty due to a low number of fatigue and manoeuvre load tests. (Result for seven available fatigue tests and fifteen instances per manoeuvre)

5 VALIDATION OF SUBSTANTIATION MODELS

5.1 Synthetic reference problem

Validation on a real fatigue life prediction case is fundamentally impossible due to the extremely large sample sizes that would be required, e.g. to define the real fatigue life. Therefore, the analytical and simulation-based fatigue life prediction substantiation models are both tested on a synthetic reference problem for which the ‘true’ fatigue life distribution can be simulated. This reference case is designed to be realistic but is not specific for any particular helicopter component.

The definition of the S-N-P curve is as in Figure 5.1. The strength factor standard deviation is set to a realistically low value to maximize the relative influence of variance in

loads on fatigue life. This is important as the simulation-based model is meant to improve accuracy by explicitly accounting for the influence of uncertainty in loads on fatigue life.

Random synthetic flight regimes are used to do ‘virtual manoeuvre load testing’. A Fourier series is used to form a random load signal for the i^{th} synthetic regime of the i^{th} virtual manoeuvre load test:

$$(3.11) \text{ [Load signal]}_i = \sum_{n=1}^k a_{i,n} \sin(f_{i,n} \cdot t + \phi_{i,n}) + m_{i,n}$$

For each manoeuvre, random manoeuvre type parameters set a multivariate normal distribution. $K = 5$ signal parameters are randomly drawn from the distributions that these random manoeuvre type parameters define, each time a virtual manoeuvre load test is performed:

$$(3.12) [a_i, f_i, \phi_i, m_i] = N\left(\left[\mu_{a,i}, \mu_{f,i}, \mu_{\phi,i}, \mu_{m,i}\right], \left[\sigma_{a,i}, \sigma_{f,i}, \sigma_{\phi,i}, \sigma_{m,i}\right]\right)$$

To define the virtual flight manoeuvres, ‘type’ parameters for $i = 15$ different manoeuvres are randomly drawn from uniform and/or normal distributions, for example:

$$\mu_m = U[-10,10] \cdot 2.7 \quad \sigma_m = N(0,1) \cdot 1.4$$

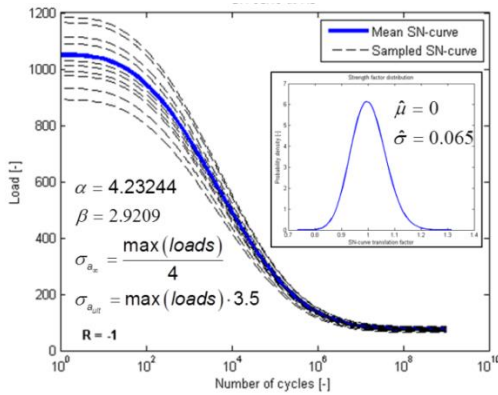


Figure 5.1: Definition the S-N-P curve in the reference problem. See also equations (2.1) and (2.5). “Loads” refers to all sampled load signals, as in Figure 5.2.

Some load signals from this random flight regime model are shown in Figure 5.2. Corresponding distributions for regime minimum and maximum load are given in Figure 5.3. Figure 5.4 then shows corresponding regime damage distributions, computed with strength factors according to the distribution defined in Figure 5.1.

The mission profile is randomly defined by drawing a random sequence of 150 flight regimes and setting the regime timeshare proportional to the number of occurrences of the regime in the random sequence. Figure 5.5 shows an example of a drawn sequence of manoeuvre extreme loads.

Defining a reference problem in this way allows doing a virtually infinite number of flight and fatigue tests. For a randomly generated problem, it is thus possible to very accurately simulate the ‘true’ distribution of fatigue life by simple BMC simulation. Figure 5.6 shows such a reference fatigue life distribution. All the reference distributions that are used for validation contain 10^5 samples. The CoV of the ‘true’ P_{fail} of the ‘true’ 10^{-3} lifetime quantile is then 10% (according to (3.6)). This means that it is roughly 99.7% certain that the P_{fail} of the ‘true’ 10^{-3} lifetime quantile is actually between $1.3 \cdot 10^{-3}$ and $0.7 \cdot 10^{-3}$. This imprecision must be considered when regarding observed estimation errors of the models.

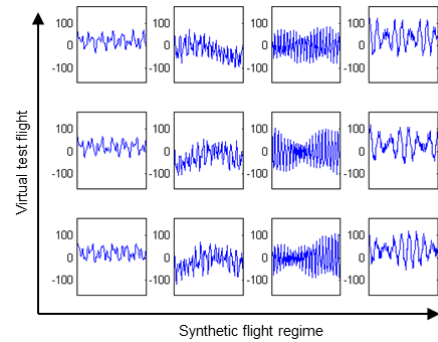


Figure 5.2: Example of artificially generated test flight data. Note the similarity between samples for the same regime and the difference between the regimes.

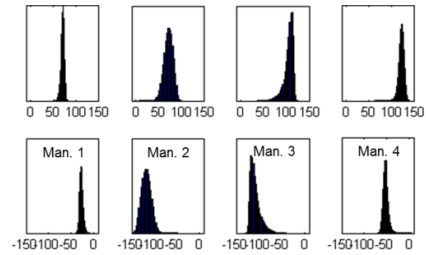


Figure 5.3: Example of reference flight regime maximum (above) and minimum (below) load (marginal) distributions

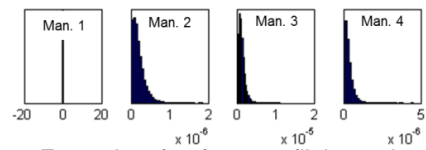


Figure 5.4: Example of reference flight regime damage (marginal) distributions

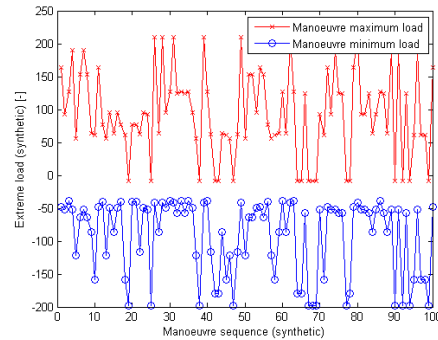


Figure 5.5: Example of sampled GAG extreme manoeuvre loads before extreme load and PV-filtering.

5.2 Verification test under idealized circumstances

First, the ideal performance of the standard analytical (section 2) and new simulation-based (section 4) fatigue life substantiation models are tested to see if these models are asymptotically correct. Ideal conditions are defined as having $5 \cdot 10^5$ fatigue tests and 10^4 flight tests available. Hence, if a model makes wrong estimates, then this must be due to fundamental shortcomings in the model itself, as there is practically no uncertainty in the fitted strength and load distributions that serve as input to the models.

5.2.1 Standard analytical method

The standard method is tested by using the ‘true’ lifetime distribution to compute the actual P_{fail} of the lifetime quantile that the standard method predicts. As in Figure 5.6, this actual P_{fail} is about $7 \cdot 10^{-3}$, i.e. the failure probability of the predicted lifetime is about seven times higher than the target of 10^{-3} . This indicates that the standard reliability substantiation model is, under ideal circumstances, inaccurate and non-conservative. The cause is that the standard method only computes with the average (extreme) loads and neglects effects of their variance.

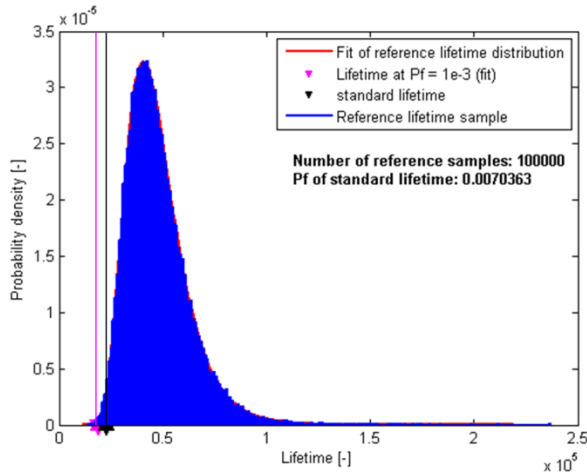


Figure 5.6: Comparison between the (synthetic) 10^{-3} lifetime quantile according to the reference distribution and the standard prediction method.

5.2.2 Simulation-based method

The new simulation-based fatigue life substantiation model is tested differently as it does not directly predict a lifetime percentile. It is only tested if the new model indeed predicts a 10^{-3} probability of failure for the lifetime that is already known to be the 10^{-3} quantile of the ‘true’ reference lifetime distribution. As in Figure 5.7, the predicted $P_{fail}(SLL_{ref})$ is $1.05 \cdot 10^{-3}$. This is practically a perfect result, as the estimate is well within an approximate ‘one sigma’ confidence interval of the ‘true’ reference quantile. The test result therefore provides very strong evidence that the newly proposed fatigue life substantiation model is asymptotically correct. This is in contrast to the standard model.

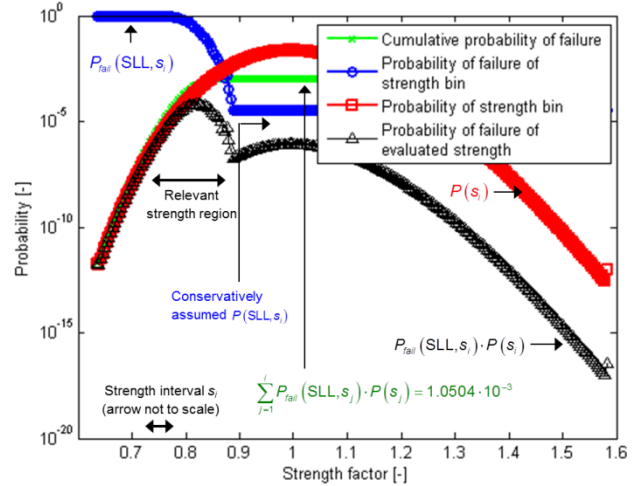


Figure 5.7: SS results under ideal circumstances. The circles in the blue line show $P_{fail}(SLL_{ref})$ for the i^{th} strength interval. Note that this failure probability is conservatively assumed for most intervals as this probability approaches zero as strength goes up (i.e. practically none of the components fails before the SLL for strength factors higher than about 0.9). The probability of having a component in the i^{th} strength interval is displayed by the squared red line. The triangulated black line shows the point-wise multiplication between P_{fail} given strength and the probability of this given strength. The dotted green line finally shows the cumulative probability of failure, which here accumulates to $1.05 \cdot 10^{-3}$. The computation was executed with 10^3 samples per subset and a strength distribution discretized in 250 intervals (Hence a very accurate but computationally expensive configuration).

5.3 Validation test with realistic small samples

In practice, the number of tests that can be done is small and computational resources are limited. Therefore, the validation tests are repeated but now while assuming that only seven fatigue tests have been done and that every flight regime was only test-flown fifteen times. Computational costs are limited by dividing the strength distribution in wide intervals and by using low number of samples per subset distribution.

It can now no longer be expected that any of the models perfectly predicts the 10^{-3} fatigue life percentile. The small amount of test results available to make a prediction does not give a perfect representation of the ‘true’ load and strength distributions and thus causes inevitable errors. Instead, it is tested if the models give a conservative estimate of the 10^{-3} fatigue life quantile in 95% of the cases.

5.3.1 Standard method

Figure 5.8 shows 250 repetitions of estimating the same conservative lifetime quantile with the standard method. Seven virtual fatigue tests and fifteen virtual tests per manoeuvre were newly performed per repetition. It shows that if no confidence interval would be computed, only about 40% of the lifetime predictions would actually meet the $1 \cdot 10^{-3}$ reliability requirement. This can be understood

by noting that the estimator of the variance, most notably of fatigue strength, is biased towards underestimating the variance. The error in the estimate of the true standard deviation σ is proportional to $\sigma/(4 \cdot n_{test})$. Simulations confirm that it is 'normal' to underestimate the standard deviation in about 60% of the cases if only seven tests are done. In case of the standard fatigue life prediction method this automatically means that the lifetime percentile is non-conservatively overestimated in 60% of the cases, as strength dominates the prediction. However, Figure 5.8 shows that if the 10^{-3} lifetime quantile is computed with a single-sided 95% confidence interval, then the method is successful in achieving the targeted confidence level. Only 9 out of 250 of repeated predictions failed to meet the $1 \cdot 10^{-3}$ reliability requirement, showing a realized confidence level of 96.4%.

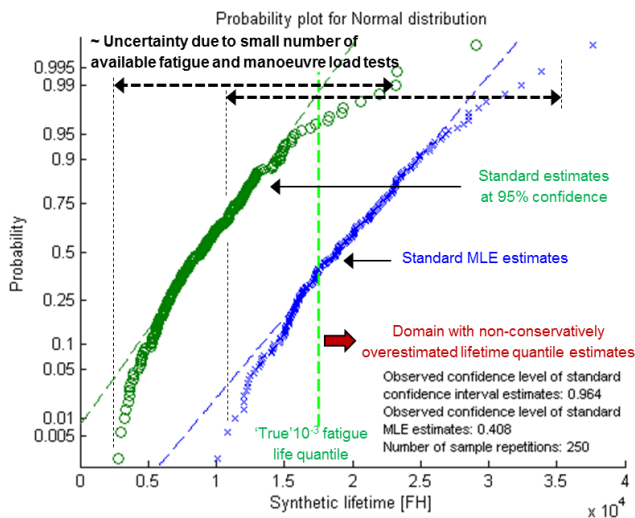


Figure 5.8: Testing of the standard fatigue life prediction method for realistically small samples.

The test as in Figure 5.8 was repeated 25 times for redrawn synthetic problems to increase confidence in the accurate behavior of the standard method. The distribution of the realized confidence levels is shown in Figure 5.9. Considering that the 'one-sigma' confidence intervals of the realized confidence levels themselves have an approximate width of 2.8%, then it may be concluded that the standard method yields practically perfect estimates, at least for the tested problem family. To even further increase confidence in the accuracy of the standard method, the test as in Figure 5.9 is repeated but while simulating that 'only' seven, instead of fifteen, manoeuvre load tests were performed per manoeuvre. So the relative uncertainty in estimated manoeuvre loads is increased. The realized confidence levels followed a comparable normal distribution as in Figure 5.9 but with slightly increased variance (imprecision). This means that the error that the method generally makes by neglecting any effects of uncertainty in loads is in practice not significant in comparison to the effects of uncertainty in strength, which is duly accounted for.

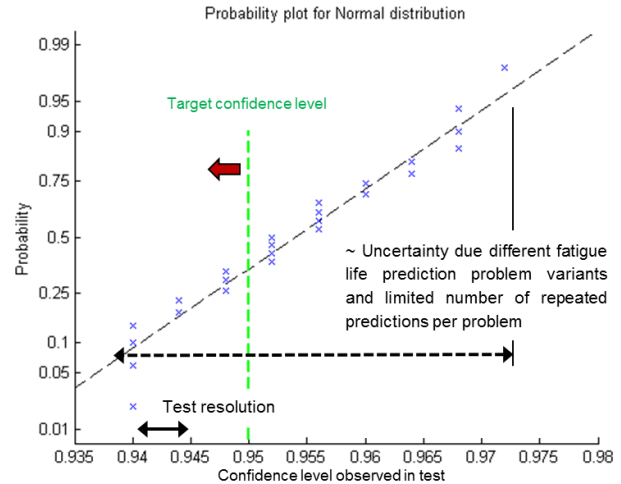


Figure 5.9: Repeated testing of the standard fatigue life prediction method for realistically small samples.

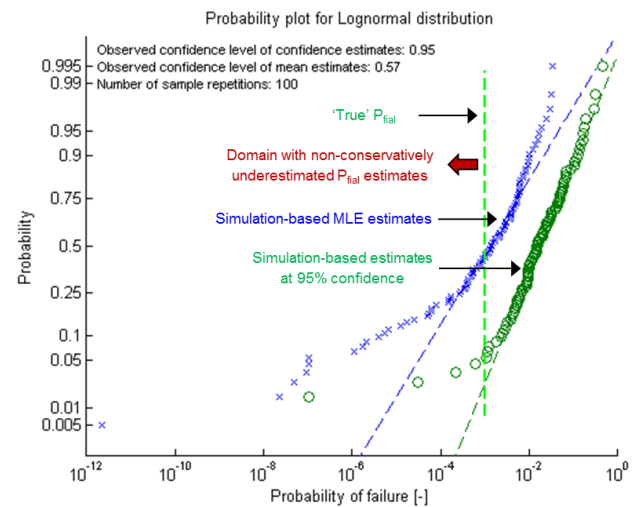


Figure 5.10: Testing of the simulation-based fatigue life substantiation model for realistically small samples. The simulation used 150 samples per subset, a strength distribution discretized in 25 intervals and 25 bootstraps per repeated sample. (Hence a computationally 'cheap' configuration).

5.3.2 Simulation-based method

The new simulation-based method is first tested by checking if it indeed predicts a 10^{-3} probability of failure for the lifetime that is already known to be the 10^{-3} quantile of the 'true' reference lifetime distribution. The predicted P_{fail} may not be lower than 10^{-3} for 95% of the load and strength sampling repetitions when the method targets a 95% single sided confidence interval. Figure 5.10 shows that 5/100 of the repeated predictions were too optimistic regarding the probability of failure of the true 10^{-3} lifetime quantile. This is practically 'perfect' performance when considering the precision of this 'true' reference. The test as in Figure 5.10 is also repeated while simulating that 'only' seven manoeuvre load tests were performed per manoeuvre. Then, 89/100 MLE estimates and 99/100 upper confidence level estimates were observed to meet the actual reliability requirement. This too conservative result is believed to be caused by an over conservatively

designed custom procedure that hedges practical issues in fitting multi-dimensional distributions through few sample points. The authors are confident though, that a simple adjustment in the fitting procedure will yield more accurate results.

The practical engineering problem is however not to predict P_{fail} of a given lifetime but rather to predict a lifetime that meets a reliability requirement (i.e. $1-10^{-3}$). Hence, a custom Reliability Based Design Optimization (RBDO) application was developed to use the simulation-based lifetime substantiation model to ‘design’ lifetimes that meet a reliability requirement. Figure 5.11 shows an illustrative result from the RBDO application.

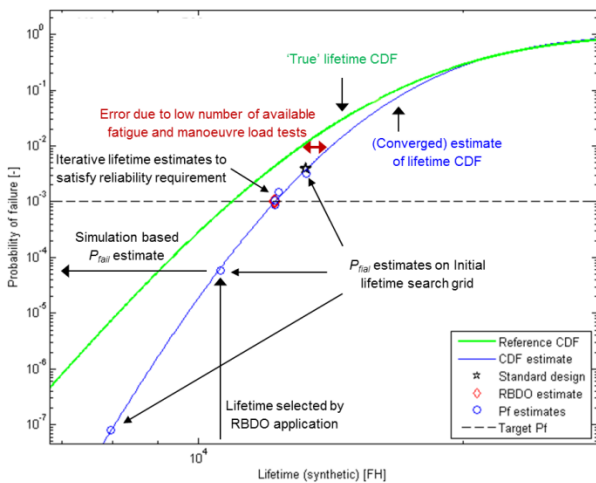


Figure 5.11: Illustrative result from a custom developed RBDO application to predict fatigue life using the simulation-based fatigue life substantiation model. Note that P_{fail} estimates around the same lifetime do not differ much, demonstrating the high precision of SS in the newly proposed method (i.e. with 150 samples per subset).

Figure 5.12 shows 50 repetitions of estimating the same conservative lifetime 10^{-3} lifetime quantile with the custom RBDO application, while having only seven fatigue and fifteen manoeuvre load tests available. It shows that none of the repeated lifetime designs fell below the ‘true’ 10^{-3} lifetime quantile. As a 95% upper single sided confidence level was targeted, this test clearly demonstrates too conservative results. The validation test of the simulation-based $P_{fail}(SLL)$ estimates, as in Figure 5.10, was passed successfully. Therefore, the authors are confident that manageable adjustments of the RBDO application will yield more accurate results.

5.3.3 Simultaneous comparison

The results in Figure 5.12 also allow direct comparison between the simulation-based and analytical method. The test result demonstrates that lifetime quantiles designed by the simulation-based method are similar to estimates from the standard method, though somewhat over-conservative. In general though, it therefore seems that, for the tested problem family and with realistically small

sample sizes, the ideally attainable precision in estimating a reliable lifetime is simply governed by the precision up to which a quantile of a lognormal strength distribution can be estimated.

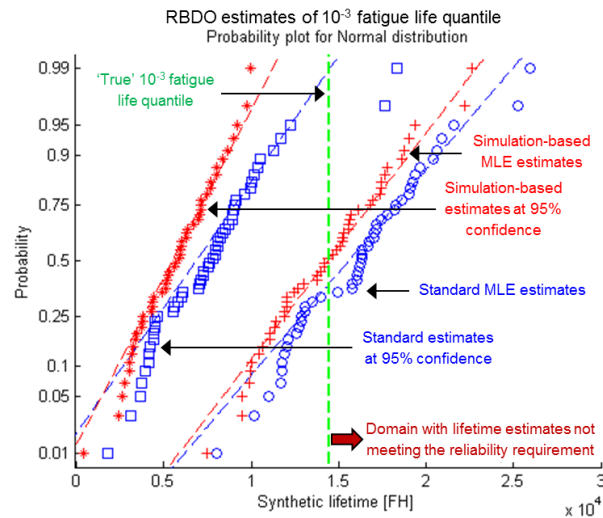


Figure 5.12: Testing of both the simulation-based and standard fatigue life quantile prediction models. (The simulation used 150 samples per subset, a strength distribution discretized in 20 intervals and 25 bootstraps per repeated sample.)

6 CONCLUSIONS

It is demonstrated that a fundamental and non-conservative error is made when the reliability of a predicted fatigue life is substantiated using only the distribution of fatigue strength and simplifying the flight manoeuvre load distributions to their mean values. A new simulation-based fatigue life prediction method was successfully validated and was shown to yield accurate results under all tested conditions.

Strikingly however, it is also demonstrated that the standard method does nevertheless feature practically perfect performance under all tested *and realistic* engineering conditions. Direct comparison under these realistic conditions between the standard analytical and simulation-based method actually revealed no practically significant differences in precision. This means that under small sample size conditions, uncertainties in manoeuvre loads may be fully neglected and the full reliability substantiation may be derived from the fatigue strength distribution only.

As the standard analytical method is much easier (and cheaper) to apply it is therefore recommended to only resort to the new simulation-based method when circumstances are encountered that clearly indicate that variance and uncertainties from manoeuvre loads are no longer insignificant in comparison to variance and uncertainty from fatigue strength. (i.e. in situations where it is precisely known that strength has a very low variance but where loads are still quite uncertain)

REFERENCES

- [1] J. Schijve, *Fatigue of Structures and Materials*, 2nd ed.: Springer Science+Business Media, 2009.
- [2] G. J. Hahn and W. Q. Meeker, *Statistical Intervals: A Guide for Practitioners.*: John Wiley & Sons Inc., 1991.
- [3] A. Wald and J. Wolfowitz, "Tolerance Limits for a Normal Distribution," *The Annals of Mathematical Statistics*, vol. 2, pp. 208-215, June 1946.
- [4] D.C. Lombardo and K.F. Fraser, "Importance of Reliability Assessment to Helicopter Structural Component Fatigue Life Prediction," DSTO Aeronautical and Maritime Research Laboratory, Fishermans Bend, Victoria, Australia, Technical Note DSTO-TN-0462, 2002.
- [5] A. E. Thompson and D. O. Adams, "A computational method for the determination of structural reliability of helicopter dynamic components," in *American Helicopter Society Annual Forum*, Washington D.C., 1990, Sikorsky Aircraft Corporation.
- [6] J. Zhao, "Development and Demonstration of Advanced Structural Reliability Methodologies for Probabilistic fatigue Damage Accumulation of Aerospace Components," Sikorsky Aircraft Corporation, 2008.
- [7] Dr. J. Zhao and D.O. Adams, "Achieving Six-Nine's Reliability Using an Advanced Fatigue Reliability Assessment Model," in *American Helicopter Society 66th Annual Forum*, Phoenix, Arizona, 2012, Sikorsky Aircraft Corporation.
- [8] R. E. Jr. Benton, "Double-Linear Cumulative-Damage Reliability Method," in *American Helicopter Society 67th Annual Forum*, Virginia Beach, VA, 2011, US Army Aviation Engineering Directorate.
- [9] J. Tang and J. Zhao, "A practical approach for predicting fatigue reliability under random cyclic loading," *Reliability Engineering and System Safety*, no. 50, pp. 7-15, June 1995.
- [10] C. L. Smith and Jung-Hua, Ph.D Chang, "Fatigue Reliability Analysis of Dynamic Components with Variable Loadings without Monte Carlo Simulation," in *American Helicopter Society 63rd Annual Forum*, Virginia Beach, Virginia, 2007.
- [11] S. Moon and N. Phan, "Component Fatigue Life Reliability with Usage Monitor," in *American Helicopter Society 63rd Annual Forum*, Virginia Beach, Virginia, 2007.
- [12] M. A. Brown and Jung-Hua, Ph.D Chang, "Analytical Techniques for Helicopter Component Reliability," in *American Helicopter Society 64th Annual Forum*, Montreal, Canada, 2008.
- [13] S. Dekker, S. Bendisch, and F. Hoffmann, "Fatigue management system and method of operating such a fatigue management system," EP275337 A1, October 24, 2012.
- [14] C. Genest and A.-C. Favre, "Everything You Always Wanted to Know about Copula Modeling but Were Afraid to Ask," *Journal of Hydrologic Engineering*, vol. 12, pp. 347-368, July 2007.
- [15] J. E. Hurtado, *Structural Reliability - Statistical Learning Perspectives*, 1st ed., Prof.Dr.-Ing. Friedrich Pfeiffer and Prof.Dr.-Ing Peter Wriggers, Eds. Berlin Heidelberg, Germany: Springer-Verlag, 2004.
- [16] B. Echard, N. Gayton, and M. Lemaire, "AK-MCS: An active learning reliability method combining Kriging and Monte Carlo Simulation," *Structural Safety*, no. 33, pp. 145-154, 2011.
- [17] V. Caron, A. Guyader, M. M. Zuniga, and B. Tuffin, "Some recent results in rare event estimation," *ESAIM Proceedings*, no. 44, pp. 239-259, January 2014.
- [18] Siu-Kui Au and J. L. Beck, "Estimation of small failure probabilities in high dimensions by subset simulation," *Probabilistic Engineering Mechanics*, no. 16, pp. 263-277, 2001, California Institute of Technology - Division of Engineering and Applied Sciences.
- [19] T. Hesterberg, D. S. Moore, S. Monaghan, A. Clipson, and R. Epstein, *Introduction to the Practise of Statistics - 6th edition.*: W.H. Freeman, 2009, ch. 16.

COPYRIGHT STATEMENT

The author(s) confirm that they, and/or their company or organisation, hold copyright on all of the original material included in this paper. The authors also confirm that they have obtained permission, from the copyright holder of any third party material included in this paper, to publish it as part of their paper. The author(s) confirm that they give permission, or have obtained permission from the copyright holder of this paper, for the publication and distribution of this paper as part of the ERF2014 proceedings or as individual offprints from the proceedings and for inclusion in a freely accessible web-based repository.